Probing the luminescence of single Eu2O3 nano-islands on MgO(001) with scanning tunneling microscopy

Fernando Stavale, Niklas Nilius, and Hans-Joachim Freund

Probing the luminescence of single Eu$_2$O$_3$ nano-islands on MgO(001) with scanning tunneling microscopy

Fernando Stavale, Niklas Nilius,[a] and Hans-Joachim Freund

Fritz-Haber-Institut der Max-Planck-Gesellschaft, Faradayweg 4-6, D-14195 Berlin, Germany

STM imaging and cathodoluminescence spectroscopy are used to explore the morphology and optical properties of Eu$_2$O$_3$ nano-islands grown on MgO(001) thin films. The global emission properties are governed by intense photon peaks at around 600 nm, arising from forced-dipole transitions in the 4f-state manifold of Eu^{3+} ions placed in a non-centrosymmetric crystal field. Local optical spectra obtained in the tunneling mode of the STM reveal that the Eu$_2$O$_3$ islands are responsible for the distinct optical response and not isolated Eu^{3+} ions inside the MgO matrix. Our work demonstrates that thin-film model systems can be used to elucidate fundamental properties of Eu-containing phosphors on the nanometer scale. © *2012 American Institute of Physics*. [http://dx.doi.org/10.1063/1.4731638]

Compound materials doped with rare-earth (RE) metal-ions play an important role in various fields of science and technology, such as fuel cells,[1] gas- and bio-sensors,[2,3] light-emitting devices,[4] and heterogeneous catalysts.[5] Particularly interesting are the luminescence properties of RE-metals diluted in oxide matrices, e.g., of Eu, Gd, and Er in Y$_2$O$_3$ and Gd$_2$O$_3$ hosts,[6] which form the basis for highly efficient phosphors with tunable emission properties. Their distinct optical behavior is governed by electron transitions inside the 4f-state manifold of the RE-ions that give rise to sharp and intense optical bands. The atom-like emission characteristic of RE-impurities is owed to the strong shielding of the 4f orbitals by the outer 5sp shell, resulting in energetically and spatially confined states with little overlap to neighboring levels. The emission behavior of Eu-containing phosphors, in particular, is dominated by transitions between the ^{5}D$_0$ initial and different ^{7}F$_J$ final states with the total orbital-momentum quantum number J running from 0 to 6.[7] The associated bands are centered at around 600 nm and thus responsible for the intense red color of Eu-phosphors.

RE-compounds have been intensively studied as powder samples, using x-ray diffraction and electron microscopy for structural and morphological analyses and luminescence spectroscopy for optical characterization.[7–9] These techniques are sensitive only to bulk properties of the (crystalline parts of the) material and average over large numbers of optically active entities with different composition and binding environment. Deeper insight into the nature of the emission centers, as typically deduced from electron-spectroscopy and microscopy, cannot be acquired on powder samples due to their insulating character and complex morphology. Moreover, the role of the surface is widely disregarded although surface properties become decisive if not the optical but the chemical behavior of the RE-compounds is in the focus of research.

In this study, we have developed a surface-science-compatible model for a RE-system,[10] comprising Eu$_2$O$_3$ nano-islands on a thin MgO film grown on a Mo(001) support. Due to the conductive nature of our samples, we were able to employ scanning tunneling microscopy (STM) and

low-bias cathodoluminescence (CL) spectroscopy for the morphological and optical characterization of single luminescent centers, respectively. Owing to the high spatial resolution of our method, we can demonstrate that Eu$_2$O$_3$ nano-islands and not single Eu dopants inside the MgO matrix are responsible for the characteristic red light emission of our samples.

The experiments have been performed in a specifically designed, ultra-high vacuum STM operated at 100 K.[11] A Beetle-type STM head has been placed inside a parabolic mirror that collects photons from the tip-sample junction. A second mirror outside the vacuum refocuses the light onto the entrance slit of a spectrograph equipped with 150 and 600 lines/mm gratings attached to a charge-coupled device (CCD). CL-spectroscopy has been performed by slightly retracting the STM-tip from the surface and applying bias voltages of −7 and −200 V for local and non-local measurements, respectively. The electron current was adjusted to 5 nA using the feed-back loop of our STM. The outgoing photons were accumulated for 300 s by the CCD detector. In order to exclude electron-induced damage, we have imaged the probed surface region before and after each spectral run.

The MgO films used as support were prepared by reactive Mg deposition onto a clean Mo (001) single crystal in 5×10^{-7} mbar O$_2$ followed by vacuum annealing to 1000 K.[12] The film thickness was fixed to 10 and 50 ML for STM and high-resolution CL-measurements, respectively. In both cases, low-energy-electron diffraction data displayed a sharp (1×1) square pattern, as expected for rocksalt MgO(001).[12] STM images of thin-film samples indicated an atomically flat surface, comprising rectangular terraces of 10-20 nm size separated by [100]-oriented dislocation lines (Fig. 1(a)). The so prepared films were exposed to 0.5 ML Eu, resulting in the growth of 3D metal particles bound to the MgO line defects. To transform the optically inactive metal deposits into optically active centers, the samples were annealed in 5×10^{-7} mbar O$_2$ at 800 K for 10 min. During this procedure, the metal particles vanished, partly due to evaporation into the gas phase and partly due to Eu incorporation into the oxide film (Fig. 1(b)). However, the initial MgO morphology did not recover as a high density of planar,
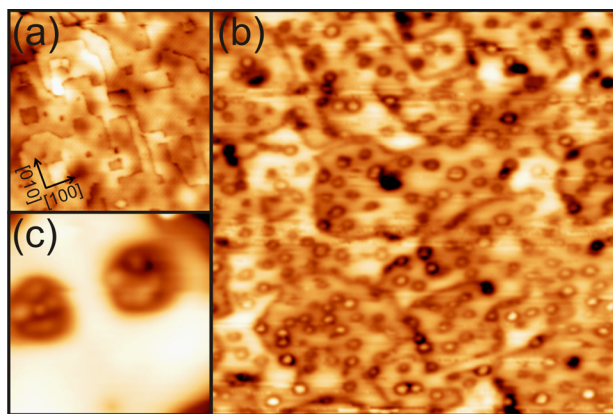
a)E-mail: nilius@fhi-berlin.mpg.de.

FIG. 1. (a) STM topographic image of a bare 10 ML thick MgO film on Mo(001) ($100 \times 100\,nm^2$). (b) Image of Eu_2O_3 nano-islands produced by depositing 0.5 ML Eu onto MgO and annealing in O_2 ($100 \times 100\,nm^2$). (c) Close-up of two Eu_2O_3 islands located on an MgO terrace ($15 \times 15\,nm^2$).
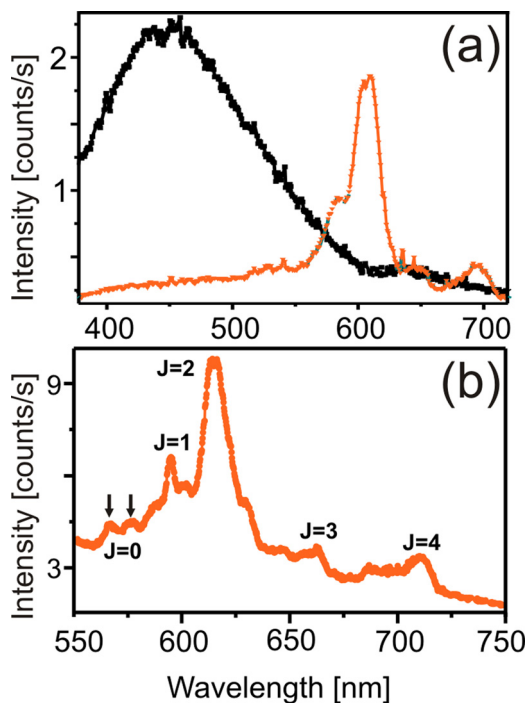

FIG. 2. (a) CL-spectra of bare (black) and Eu_2O_3-covered (orange) MgO taken at 200 eV electron energy. (b) High resolution spectrum of the Eu-MgO system with the different J transitions being indicated. The splitting of the $J = 0$ peak is marked by arrows.

3-5 nm wide islands appeared on the surface. Their position coincides with the former nucleation sites of the metal particles, i.e., most of them are found on the dislocation network and only a few on the MgO terraces. The island interior is made up of several irregularly spaced maxima being surrounded by a dark ring (Fig. 1(c)). We exclude a metallic nature of the ad-islands as metal deposits are typically imaged as protrusions and not as faint depressions as found here. We rather suggest that the Eu becomes fully oxidized upon O_2 exposure, adopting the thermodynamically preferred Eu_2O_3 stoichiometry.[13] Assuming a mono-layer height, we can estimate the number of Eu^{3+} ions in each surface-island to be around fifty.

The ultimate method to analyze the nature of the MgO-supported islands is optical spectroscopy,[7,14] accomplished by means of CL-measurements in our case. The optical signature of pristine MgO films is governed by a broad maximum at 400 nm (Fig. 2(a)), being ascribed to the radiative decay of excitons trapped at three-fold coordinated O-sites in the MgO surface.[15,16] The emission disappears upon Eu exposure as the exciton-recombination centers get blocked by the metal particles. After annealing in O_2, a new peak emerges at ~615 nm which matches the reported optical signature of Eu^{3+} in different insulating hosts.[6–8] The comparable emission response supports our assumption that small Eu_2O_3 grains have formed on the MgO film during the high-temperature oxidation of the Eu particles. High resolution CL-spectra acquired on 50 ML thick MgO films provide additional insight into the nature of the Eu^{3+} emission centers (Fig. 2(b)). Five sets of photon bands are resolved between 550 and 725 nm, being assigned to transitions between the $^5D_0$ excited and the ^7F_J final states of Eu^{3+} with J running from 0 to 4. Their centers of gravity have been determined to be 566 nm ($J = 0$), 595 nm ($J = 1$), 615 nm ($J = 2$), 662 nm ($J = 3$), and 710 nm ($J = 4$) with the $J = 2$ peak being the most intense. Apart from $J = 1$, all Eu^{3+} transitions are dipole forbidden in the free ion and become detectable only upon symmetry reduction in a local crystal field acting on the embedded species. The $J = 2$ transition is enabled by odd-parity components of the crystal field, which trigger a mixing of the Eu $4f$ and $5d$ levels and stimulate hybridization among the different $4f$ orbitals.[9] The high in-

tensity of the $J = 2$ peak thus indicates a large number of Eu^{3+} ions in sites without inversion symmetry. This condition is fulfilled basically for all Eu^{3+} in the surface islands, as those interact simultaneously with ligands in the MgO and the Eu_2O_3 and are hence subject to a non-centrosymmetric crystal field. Further information comes from the fine-structure of the different J-transitions. For each unique Eu^{3+} site in the sample, one $J = 0$ but up to three $J = 1$ peaks are expected to occur, given the $(2J + 1)$ degeneracy of the J manifold.[7] However, already the $J = 0$ transition is split into two maxima at 567 and 576 nm, indicating the presence of two non-equivalent Eu^{3+} sites in our samples (arrows in Fig. 2(b)). An obvious assignment would be to Eu^{3+} ions located either at the perimeter or in the interior of the Eu_2O_3 islands. Alternatively, different Eu^{3+} species might be present inside the clusters, reflecting the different local Eu^{3+} binding environment in cubic and monoclinic Eu_2O_3. Finally, single Eu^{3+} ions within the MgO lattice may contribute to the signal although we consider Eu diffusion into the MgO film unlikely because of the large Eu^{3+} ion radius with respect to the MgO lattice parameter.[17]

The latter possibility can be excluded also on the basis of local CL-experiments performed in the tunneling mode of the STM. Due to the small tip-sample distance at 7.0 V excitation bias, the spatial resolution of our spectroscopy increases to ~1 nm and the optical response of pristine MgO and Eu_2O_3 nano-islands can be probed separately (Fig. 3).[18,19] For tip positions above the bare film, the emission is governed by a peak at 700 nm that is not intrinsic to MgO but relates to a tip-mediated emission channel.[20] It arises from radiative electron-transitions between so-called field emission resonances (FERs),[21] being vacuum states that develop in the classical region of the tip-sample junction at high bias voltages.
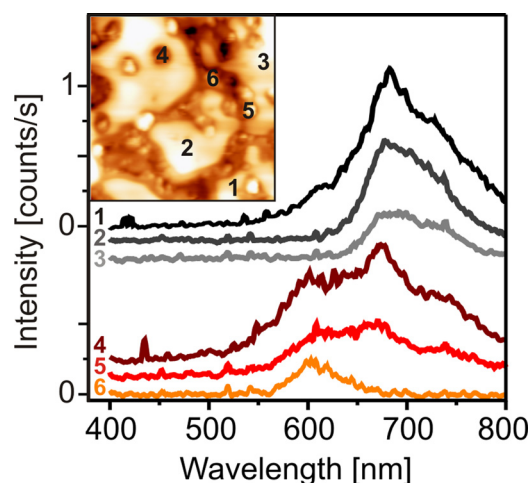
FIG. 3. Local luminescence spectra taken at 7.0 V sample bias and 5 nA current on a Eu_2O_3-covered MgO thin film. Curves are offset for clarity. Tip positions for spectroscopy are indicated in the STM image shown in the inset (40×40 nm^2).

The resonance condition is fulfilled when the wave-packets of incoming electrons interfere constructively with the ones reflected at the sample surface and quasi-bound electronic states form in front of the MgO. Electrons being injected into these FERs have relatively long residence times due to the insulating nature of the oxide film beneath and experience an enhanced probability for radiative recombination into lower levels. The 700 nm-emission originates from electron transitions between the 2nd and 1st FER, and even the 3rd to 1st transition can be detected as a peak at 500 nm at higher excitation bias.[20] Placing the tip above a Eu_2O_3 island located either on a terrace or a dislocation line gives rise to a new peak at ∼600 nm, which matches the wavelength position of the Eu^{3+} lines. Simultaneously, the 700 nm-peak fades away as the increased roughness of the Eu-covered areas destroys the resonance condition for the FERs. Above larger Eu_2O_3 grains, the intensity of the 600 nm-line even exceeds the one of the FER-mediated peak. Still, no fine-structure can be resolved because of the notoriously low emission yield that forces us to work with large monochromator slit widths. Two aspects make us believe that this photon band originates indeed from electron transitions inside the 4f state-manifold of the Eu^{3+} ions. Its shape reproduces the envelope of the J transitions in the high-bias spectra, and, the peak exclusively appears for tip-positions above the Eu_2O_3 nanostructures and not above plain MgO. We thus conclude that Eu-containing islands and not single dopants inside the MgO are responsible for the emission response. This implies that the optical signature that is commonly assigned to isolated Eu^{3+} ions in different oxide hosts might be caused by Eu_2O_3 aggregates as well. In this case, radiative recombination is possible only if the loss in oscillator strength due to excitation transfer to neighboring Eu^{3+} species is small, a condition that seems to be fulfilled for our islands that contain no more than 50 Eu ions.[22]

Finally, we discuss possible excitation mechanisms of the Eu_2O_3 nano-islands. In far-field CL-spectra, the distinct Eu^{3+} peaks appear only at electron energies above 50 eV, indicating an involvement of MgO core-excitations in the emission process.[23] As those excitations are inaccessible at 7 eV-electron energy, we propose that inelastic tunneling processes in which the tip-electrons transfer energy to the Eu 4f-manifold govern the excitation in the local CL-mode. A radiative decay of the excited f-states is even more probable in this case, as the strong electromagnetic near-field in the tip-sample cavity is known to enhance the emission cross section.[18,24]

In conclusion, topographic imaging and CL-spectroscopy performed in an STM setup have been used to identify the nature of optically active centers in Eu-MgO samples. We have shown that Eu_2O_3 nano-islands, prepared by annealing metallic Eu particles in O_2, are responsible for the light emission. Position and relative intensity of the main bands, assigned to $^5D_0 \rightarrow {}^7F_J$ transitions in the 4f manifold of Eu^{3+}, were found to match the results obtained for conventional Eu-doped powder samples. This finding suggests that not only isolated Eu^{3+} species diluted in an insulating host matrix, but also Eu_2O_3 aggregates give rise to the characteristic red photon-emission of Eu-phosphors. Moreover, we have demonstrated that spatially resolved optical experiments are feasible also on dielectric films, which opens new possibilities to explore the physics and chemistry of doped oxide materials at the nano-scale.

[1]P. Furler, J. R. Scheffe, and A. Steinfeld, Energy Environ. Sci. **5**, 6098 (2012).
[2]X. Niu, W. Du, and W. Du, Sens. Actuators B **99**, 399 (2004).
[3]J. Chen, S. Patil, S. Seal, and J. F. McGinnis, Nat. Nanotechnol. **1**, 142 (2006).
[4]K. C. Teixeira, G. F. Moreira, W. G. Quirino, C. Legnani, R. A. Silva, M. Cremona, H. F. Brito, and C. A. Achete, J. Therm. Anal. Calorim. **106**, 587 (2011).
[5]V. Shapovalov and H. Metiu, J. Catal. **245**, 205 (2007); B. Li and H. Metiu, J. Phys. Chem. C **115**, 18239 (2011).
[6]G. Blasse and B. C. Grabmaier, *Luminescent Materials* (Springer, Heidelberg, 1994).
[7]S. Hüfner, *Optical Spectra of Transparent Rare Earth Compounds* (Academic, Heidelberg, 1978).
[8]D. K Williams, H. Yuan, and B. M Tissue, J. Lumin. **83–84**, 297 (1999); B. Bihari, H. Eilers, and B. M. Tissue, J. Lumin. **75**, 1 (1997).
[9]T. Qin, G. Mountjoy, N. D. Afify, M. F. Reid, Y. Y. Yeung, A. Speghini, and M. Bettinelli, Phys. Rev. B **84**, 104206 (2011).
[10]D. Förster, J. Klinkhammer, C. Busse, S. Altendorf, and T. Michely, Phys. Rev. B **83**, 045424 (2011).
[11]H.-J. Freund, N. Nilius, T. Risse, S. Schauermann, and T. Schmidt, Chem. Phys. Chem. **12**, 79 (2011).
[12]S. Benedetti, H. M. Benia, N. Nilius, S. Valeri, and H.-J. Freund, Chem. Phys. Lett. **430**, 330 (2006).
[13]K. A. Gschneidner, Jr., J. Less-Common Met. **17**, 13 (1969).
[14]B. Henderson and G. F. Imbusch, *Optical Spectroscopy of Inorganic Solids* (Clarendon, Oxford, 1989).
[15]M. Anpo, Y. Yamada, Y. Kubokawa, S. Coluccia, A. Zecchina, and M. Che, J. Chem. Soc. Faraday Trans. **84**, 751 (1988).
[16]S. Stankic, M. Muller, O. Diwald, M. Sterrer, E. Knözinger, and J. Bernardi, Angew. Chem. Int. Ed. **44**, 4917 (2005).
[17]J. Alarcon, D. van der Voort, and G. Blasse, Mater. Res. Bull. **27**, 467 (1992).
[18]R. Berndt, in *Scanning Probe Microscopy*, edited by R. Wiesendanger (Springer, Berlin, 1998), p. 97.
[19]N. Nilius, N. Ernst, and H.-J. Freund, Phys. Rev. Lett. **84**, 3994 (2000).
[20]H. M. Benia, N. Nilius, and H.-J. Freund, Surf. Sci. Lett. **601**, L55 (2007); H. M. Benia, P. Myrach, and N. Nilius, New J. Phys. **10**, 013010 (2008).
[21]G. Binnig, K. H. Frank, H. Fuchs, N. Garcia, B. Reihl, H. Rohrer, F. Salvan, and A. R. Williams, Phys. Rev. Lett. **55**, 991 (1985).
[22]A. P. Demchenko, *Introduction to Fluorescence Sensing* (Springer, Berlin, 2008), p. 91.
[23]F. Stavale, N. Nilius, and H.-J. Freund, New J. Phys. **14**, 033006 (2012).
[24]P. Johansson, R. Monreal, and P. Apell, Phys. Rev. B **42**, 9210 (1990).